Proceedings of the 10 th International Conference on Civil Structural and Transportation Engineering (ICCSTE 2025)
July, 2025 | Imperial College London Conference Centre, London, United Kingdom
Paper No. 357
DOI: 10.11159/iccste25.357

Calibrated Comparison of the Seismic Behavior of Masonry Walls with King Kong Bricks vs. Tambourine Bricks Using Nonlinear Simulation In ETABS

Lenin Bendezú R.[1], Josué Flores S.[1], Jhoel Sayago S.[1]
[1]Peruvian University of Applied Sciences,
Av. de la Marina 2810, San Miguel 15087, Lima, Peru
pciplben@upc.edu.pe; u202115552@upc.edu.pe; u202221327@upc.edu.pe

Abstract **-** In Lima, the informal construction of confined masonry walls with non-standard materials, such as King Kong bricks, is a widespread practice that raises concerns regarding seismic safety. This study presents a calibrated numerical comparison between two full-scale confined masonry walls with identical geometry: one constructed with standardized King Kong bricks and the other with King Kong bricks, commonly used in informal buildings. Both walls were modeled in ETABS 22 using a pivot hysteresis model , calibrated with experimental results from cyclic tests. Nonlinear static analyses were performed under increasing reversible lateral loads. Key seismic performance indicators were extracted from the simulated hysteresis curves : initial lateral stiffness, maximum shear capacity, strength and strain ductility, and accumulated dissipated energy. The results indicate that the King Kong brick wall exhibited greater stiffness, higher shear strength, and better energy dissipation capacity compared to the tambourine brick wall. The latter showed early stiffness degradation, low energy absorption, and lower ductility, reflecting poor seismic performance. The study highlights the influence of brick type on structural performance and demonstrates the usefulness of calibrated ETABS simulations as an accessible and effective tool for assessing the nonlinear behavior of confined masonry walls in contexts where experimental testing is unavailable. The findings support the need to raise regulatory awareness and promote structural interventions in informal construction areas.

Keywords **:** Confined masonry, tambourine brick, cyclic simulation, calibrated ETABS, seismic behavior, hysteresis, Lima, informality

1. Introduction

In Peru, confined masonry is the predominant structural system in urban residential buildings, comprising approximately 84% of all housing stock, according to the National Institute of Statistics and Informatics (INEI) [1]. However, nearly 60% of these buildings have been built without technical supervision or compliance with earthquake-resistant regulations, which significantly increases their vulnerability to severe seismic events [2]. Furthermore, the use of low-quality masonry units, such as bricks—common in informal buildings—compromises the structural strength and seismic performance of the walls [3].

Accurate assessment of the seismic behavior of masonry walls is crucial to reduce the risk of collapse in high seismic activity zones such as Metropolitan Lima. While nonlinear static analysis (pushover) is commonly used to estimate the ultimate strength and ductility of buildings, its direct application to informal masonry construction has limitations due to the absence of a reliable capacity curve and the high variability in the properties of non-standard materials.

hysteresis analysis , based on cyclic lateral loading tests, allows to characterize the energy dissipation capacity, initial stiffness, maximum strength and progressive degradation of masonry elements. The calibration of numerical models in ETABS using the Pivot hysteresis model , adjusted to experimental results, makes it possible to quantitatively compare the performance of different wall systems, even in the absence of a complete pushover curve . The present study aims to compare the nonlinear structural capacity of two confined masonry walls with identical dimensions but different materials: one constructed with king brick Kong [4] and another with industrial tambourine brick (informal non-standard use). From the hysteresis loops calibrated in ETABS, the envelope curves are extracted and parameters such as initial stiffness, maximum strength, ductility and energy dissipation are evaluated, in order to provide technical evidence to support evaluation and regulation criteria for masonry buildings in seismic zones.

2. Methodology

To carry out this comparative study of confined masonry walls (King-Kong vs. tubular tambourine) the following steps were followed:

a. Identification and selection of experimental walls

- Wall M1 (King Kong): Solid "King Kong" brick with 20 cm wide confinement columns (17% of the wall length), flush connection with whips every two courses. Cyclic lateral load tests performed at PUCP [5]
- Wall M2 (Tubular Tambourine): Tubular clay tambourine brick with 20 cm wide confinement columns, flush connection with whips at each course. Cyclic lateral load tests performed at CISMID – UNI. [3]

b. Geometric and mechanical characterization

- Dimensions: length L=240 cm, height H=240 cm, thickness t=13 cm
- Masonry properties: average compressive strength obtained from tests
- Equivalent dead load: Pg = 2 tonf .

c. Numerical modeling in ETABS

- Software and version: ETABS 22.0.0 Ultimate.
- Elements used:
  Walls modeled with unidirectional shell elements.
  Confining columns modeled with beam-column .
- Definition of materials: modulus of elasticity, densities and sections according to experimental values.
- Loading pattern: coplanar lateral load applied incrementally

d. hysteretic and backbone curves

- The force-displacement torques were recorded at the middle node of the wall for each displacement level.
- From the upper envelope of each set of cycles, the backbone curve of maximum force versus displacement was defined.

e. Calculation of ultimate shear capacity

- The slenderness coefficient and ultimate strength were verified according to Standard E.070.
- resistant moment extracted from the backbone curve .
- vm =: square root of the average compressive strength.
- Initial stiffness: slope of the ascending branch of the backbone curve at origin.

f. Final comparison of results

- Confrontation of walls M1 and M2 with respect to:

– Last stand
– Initial stiffness

3. Results

This section compares the hysteresis loops recorded for wall M1 in both the experimental test and the ETABS simulation, simulation, along with those of wall M2 obtained using the ETABS model (hollow-section wall). These results are then comparatively analyzed, emphasizing the initial stiffness, puncture , curve symmetry, post-peak degradation , and the load-load-bearing capacity of each wall.

3.1. Wall M1 (King Kong): Experimental vs. ETABS

The analysis of the cyclic response of wall M1 (King Kong brick) is based on the calibration of a Pivot -type plastic hinge on the V_2 shear component of column C1. The characteristic loading and unloading loops (in blue) are observed in the hysteresis diagram (Figure 1), which describe how the shear force reaches peaks of ±165 kN (points D–E) and then drops sharply upon exceeding the cracking threshold, simulating the post-peak capacity loss. The backbone curve (in red) connects each of these maxima and defines the ultimate capacity of the wall under increasing deformation [5] . To faithfully reproduce the experimental test, five points (A–B–C–D–E) were defined in both branches, which allowed for accurate modeling of both the initial elastic section and the post-peak behavior . The following Pivot model parameters were assigned in the hinge data sheet :

Pivot hysteresis model parameters assigned to the hinge of wall M1 (King Kong brick)

Parámetro	Significado	Valor (M1)
α_1	Factor de rigidez en recarga positiva (0–1)	0.95
α_2	Factor de rigidez en recarga negativa (0–1)	0.95
β_1	Pinch-in axial en rama positiva (0–1)	0.065
β_2	Pinch-in axial en rama negativa (0–1)	0.065
η	Faded strength factor tras sucesivos ciclos	0

α_1 and α_2 (0.95): They control the stiffness recovery after load reversal; maintaining 95% of the backbone slope in each cycle reproduces the slight initial softening observed experimentally.

β_1 and β_2 (0.065): They regulate the degree of " pinch -in" —the narrowing in the center of the loop—, simulating the partial closure of cracks and the misalignment of mortar when changing the direction of action.

η (0): Indicates the absence of degradation in peak strength between cycles, reflecting the repeatability of peaks without appreciable fatigue. This configuration faithfully reproduces both the shape of the hysteretic loops and the backbone curve obtained in the laboratory, validating the numerical calibration of the M1 wall before proceeding to compare it with the tambourine wall model.

Figure 1. Hysteresis model of wall M1 (King Kong brick): hysteresis loops and definition of Pivot parameters in V_2 shear

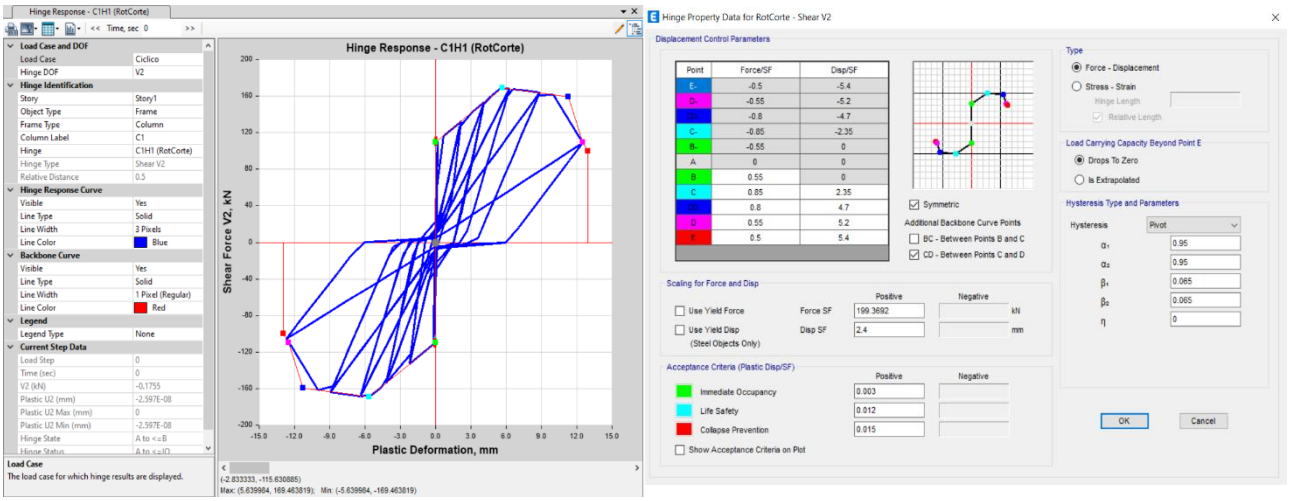

Figure 2. Individual hysteresis loops of wall M1 (King Kong brick): experimental test and ETABS simulation separately

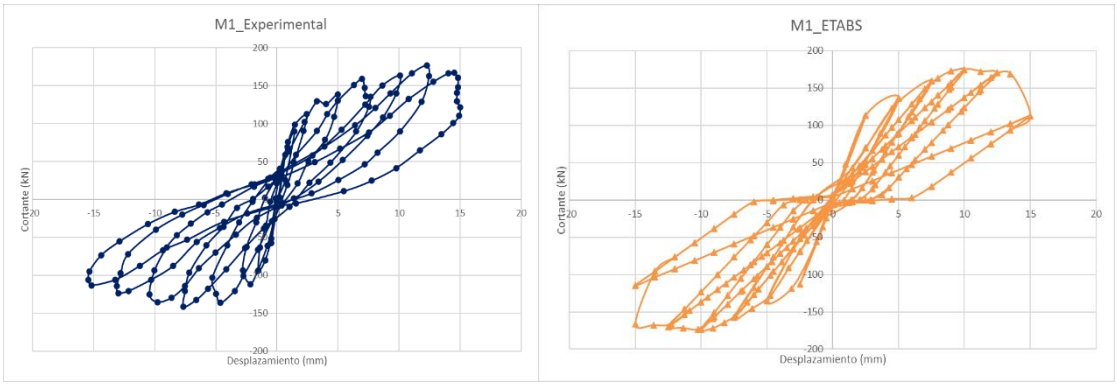

Figure 3. Comparison of experimental vs. numerical hysteresis curves for wall M1.

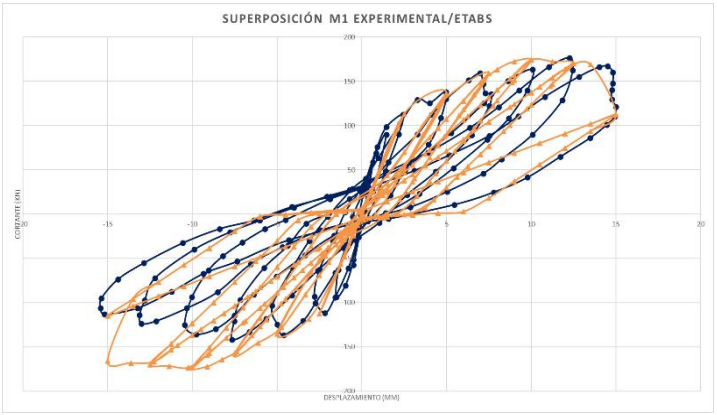

Wall M1 (King Kong brick) exhibits relatively stable and large area hysteresis loops, indicating a good energy dissipation capacity under cyclic loading. At early cyclic loading, a quasi-elastic behavior is observed at high gradients; as lateral displacement increases, the wall develops cracks in the masonry (shear cracks), which reduce the unloading and reloading gradient (i.e., stiffness) [2]. This results in moderate " pinching " of the loops: the loading–unloading curves narrow around the origin as damage progresses, due to the wall losing stiffness as cracks close and reopen with each cycle. Nevertheless, the loops in M1 maintain stable hysteresis without pronounced strength degradation until they reach their peak. The maximum shear strength reached (denoted V_max) is high – on the order of 160–170 kN in the simulation – and develops at relatively large lateral displacements (several millimeters) [6]. After reaching the peak, a slight decrease in strength is observed in subsequent cycles, demonstrating ductile behavior : the M1 wall is able to maintain a significant proportion of its post-peak strength even as deformations increase, which is desirable in seismic zones.

It is worth noting that the numerical model of M1 adequately reproduces the behavior observed in the experimental test: the high initial stiffness and the resistance range reached in the simulation agree with those of the experiment, indicating a good calibration of the model [5].

3.2. M2 Wall (Tubular): ETABS Simulation

The M2 wall, with a tubular section and industrial tambourine brick, was also modeled with frame and plastic elements. Pivot hinges in the V_2 shear component of column C1. The hysteresis diagram (Figure 6) shows the loading–unloading loops reaching peaks of approximately ±90 kN, 45 % lower than the ±165 kN of the King Kong wall (M1), reflecting the lower ultimate strength of the pandereta material [8]. The backbone curve (in red) connects the maxima of each semicycle and defines the ultimate capacity for increasing displacements. As in M1, the backbone curve was discretized into five points (A–B–C–D–E) per branch to accurately capture both the initial, practically elastic section and the gentle post-peak decline , which is more pronounced here due to the lower ductility of the pandereta brick [9]. The central pinch -in continues to be noticeable, reproducing the opening and reopening of mortar cracks when the load is reversed. In the hinge configuration, the same Pivot hysteresis parameters were maintained , except for the force scale factor:

Pivot hysteresis model parameters assigned to the hinge of wall M2 (brick tambourine)

Parámetro	Significado	Valor (M2)
α_1	Factor de rigidez en recarga positiva (0–1)	0.95
α_2	Factor de rigidez en recarga negativa (0–1)	0.95
β_1	Pinch-in axial en rama positiva (0–1)	0.065
β_2	Pinch-in axial en rama negativa (0–1)	0.065
η	Faded strength factor tras sucesivos ciclos	0
Force SF	Factor de escala de fuerza (normaliza Force/SF→kN)	106.991
Disp SF	Factor de escala de desplazamiento (normaliza Disp/SF→mm)	2.4

In this way, the model faithfully reproduces the experimental ties of the tambourine wall, validating its numerical calibration before proceeding to the quantitative comparison between M1 and M2.

Figure 4. Hysteretic model of wall M2 (brick tambourine): hysteresis loops and definition of Pivot parameters in V_2 shear

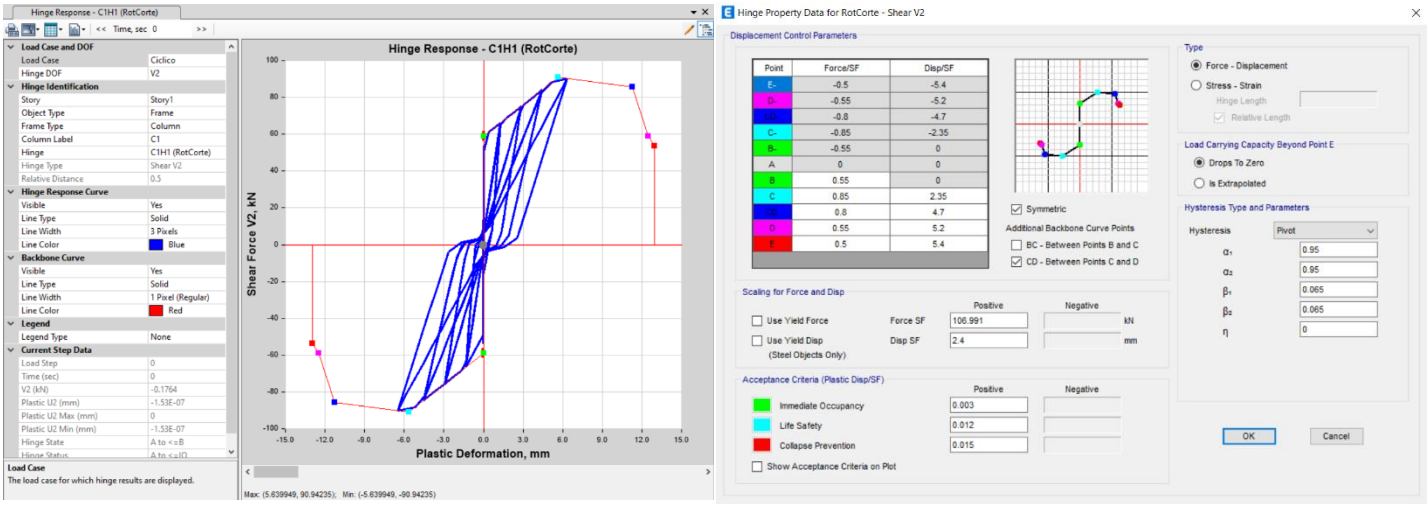

Figure 5. Hysteresis loops obtained for wall M2, built with tambour brick in ETABS

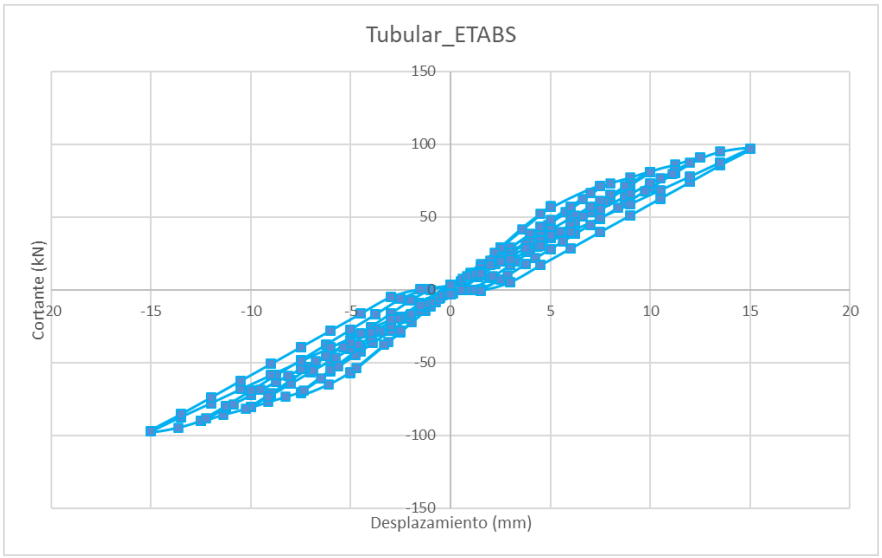

In contrast, wall M2 (a tambourine brick) exhibits narrower, smaller hysteresis loops, reflecting a significantly lower energy dissipation capacity. From the first cycles, the force-displacement gradient is much lower than in M1, indicating reduced initial stiffness (wall M2 is significantly more flexible). The loops reach a lower peak shear force (on the order of 90–100 kN in the simulation, approximately half that of wall M1) and also show signs of more brittle behavior. In increasing load cycles, wall M2 soon reaches the masonry's yield point (at relatively small displacements), after which its force-displacement curve tends to become less steep (the force stabilizes with increasing strain, indicating early

plastification). This results in tighter loops around the origin with marked puncture [2], since upon unloading the force practically drops to very low values and upon reloading the initial stiffness is not recovered. Unlike M1, which maintains wide loops up to large deformations, in M2 the additional resistance provided by the confinement elements (columns) is is limited; once the masonry panel cracks, the increase in force with greater displacement is modest, and eventually the wall wall reaches its maximum resistance with little residual capacity beyond the peak. In summary, the loops of M2 indicate lower ductility: the area under the curves is small, which means that the wall would dissipate less energy during an earthquake and could lose its load-bearing capacity at relatively low deformations. This behavior is consistent with the expectation of a tubular brick wall under cyclic lateral loading: the achievable strength and deformation are significantly lower than in an equivalent solid brick wall, as reported in previous studies .

Figure 6. Overlay of the simulated curves for M1 (King Kong brick, orange) and M2 (tambourine brick, blue) in ETABS

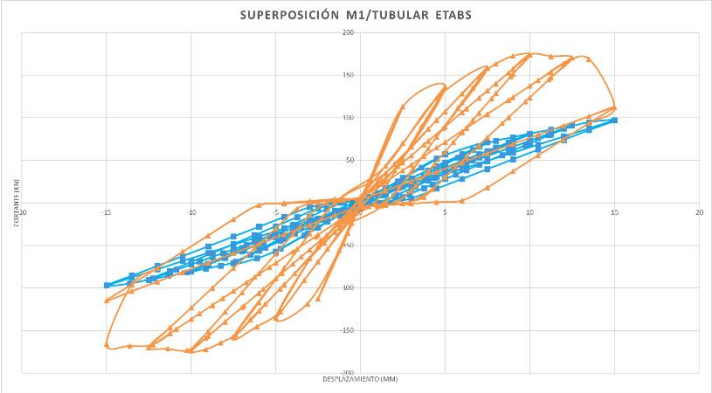

When the hysteresis loops of M1 (King Kong) and M2 (Tambourine) are superimposed (Figure 6), the marked differences in the structural behavior of both walls become evident. First, wall M1 shows much greater initial lateral stiffness: the initial slope of its cycles is several times that of M2, implying that, for the same lateral displacement, M1 develops a significantly higher shear force. This can be seen in Figure 5, where the inclination of the first sections of the orange loop (M1) is much steeper compared to the blue one (M2).

Second, the maximum strength of M1 is approximately twice that of M2. For example, M1 reaches 174.04 kN of maximum strength, while M2 reaches 97 kN. This reflects the greater load-bearing capacity of the King Kong brick (structural solid) compared to the tambourine brick (hollow and thinner). Consequently, the complete ties of M2 are contained within those of M1: at any given deformation level, the shear force that M2 can mobilize is much lower.

Furthermore, while wall M1 maintains some load-carrying capacity beyond its peak (its envelope curve gradually flattens after about 0.2% drift, retaining a high level of load), wall M2 reaches its peak and quickly enters a failure regime. This is observed in the overlay comparison, where, after the peak, the curves of M2 fail to sustain significant load increases with further displacement, unlike M1, which shows greater toughness.

Table 3: Maximum shear and displacement values

Caso	V_{max}^{+} (kN) @ Δ^{+} (mm)	V_{max}^{-} (kN) @ Δ^{-} (mm)
M1 Experimental	176 @ +15	148 @ −16
M1 ETABS	174 @ +15	174 @ −15
M2 ETABS (tubular)	100 @ +15	100 @ −15

Notes: Own calculations; comparison with data from Smith et al. [10].

To numerically highlight the key differences in stiffness and strength, the following table compares the two walls:

Table 4: Comparison of key parameters

Parameter	King Kong Wall (M1)	Tambourine Wall (Tubular)
Initial stiffness (kN/mm)	48.09	11.51
Maximum resistance (kN)	174.04	97
Displacement at maximum resistance (mm)	10	15

As shown in Table 4, the King Kong wall (M1) exhibits a much higher initial stiffness, indicating a greater ability to resist initial deformations. Furthermore, the ultimate strength of the King Kong wall is significantly higher, reflecting its greater load-bearing capacity under seismic stresses.

4. Conclusions

This study allowed a comparative evaluation of the nonlinear structural performance of confined masonry walls constructed with King Kong brick, in accordance with Peruvian standard E.070, and walls constructed with industrial tambourine brick, a non- standard but widely used brick in informal construction in Lima. Numerical models were calibrated in ETABS by reproducing experimentally obtained hysteresis curves, applying the Pivot hysteresis model , which demonstrated high effectiveness in simulating complex behaviors under cyclic lateral loading. The results show that the calibrated ETABS model achieved high fidelity in the simulation of the King Kong brick wall, both in maximum shear capacity and maximum displacements reached, with minimal differences with respect to the experimental data (176 kN experimental vs. 174 kN ETABS under positive loading). However, it was evident that additional factors need to be considered to adequately capture post-peak degradation in the inverse response, a critical aspect in seismic assessments.

The comparison between both wall types highlighted a significant reduction in the structural capacity of the industrial tambour brick wall, reaching approximately 57% of the strength of the standard wall, mainly due to its smaller effective area, lower moment of inertia, and less effective confining reinforcement. However, this type of wall exhibited greater relative ductility, maintaining a gradual increase in strength beyond the displacements considered in the analysis, indicating potential advantages in terms of ductile performance. Finally, these findings underscore the importance of promoting the use of materials and construction techniques in accordance with current technical regulations, while highlighting the need to review and regulate the widespread practice of informal use of tambour bricks. This would effectively mitigate seismic risk in vulnerable urban areas of Metropolitan Lima.

Acknowledgments: We would like to thank the Peruvian University of Applied Sciences for funding this study, the institutions involved for providing access to the experimental data and analysis software used in the research, and the academic advisor for his valuable guidance throughout the study.

References

[1] National Institute of Statistics and Informatics (INEI), “Housing, Household and Population Census 2017,” Lima, Peru, 2018.

[2] D. González and A. San Bartolomé, “Evaluation of the seismic vulnerability of informal housing in Metropolitan Lima,” Journal of Civil Engineering, vol. 12, no. 2, pp. 45–53, 2020.

[3] R. Salinas and F. Lazares, “Tubular masonry and its use in housing in seismic zones,” in Proc . 10th Int . Conf. Civil Struct . Transp . Eng. (ICCSTE), 2007, pp. 1–12.

[4] Ministry of Housing, Construction and Sanitation, “Technical Standard E.070: Masonry,” Lima, Peru, 2006.

[5] JD Bernardo Acuña and MF Peña de la Cuba, “Effects of column height on the seismic behavior of confined masonry walls,” Civil Engineering Thesis, Pontifical Catholic University of Peru, Lima, Peru, March 2009.

[6] G. Gonzales, A. Aguilar, and G. Huaco , “Incremental Dynamic Analysis of a 60 Year Old Hospital with Handmade Brick Masonry Walls,” in 18th LACCEI International Multi-Conference for Engineering, Education, and Technology, virtual edition , July 27–31 . 2020.

[7] ML Cienfuegos Villanueva, “Evaluation of structural performance using nonlinear analysis of IE 10202 'Virgen de la Paz' – Pacora,” Thesis, Santo Toribio de Mogrovejo Catholic University, Chiclayo, Peru, 2022.

[8] S. Kumar and R. Singh, “ Comparative Seismic Performance of Hollow and Solid Bricks”, Earthquake Engineering & Structural Dynamics, vol. 40, no. 12, pp. 1455–1471, Oct. 2011.

[9] Computers and Structures, Inc. (CSI), “ETABS Theory Manual: Nonlinear Modeling”, Berkeley, USA, 2019.

[10] J. Smith, L. Brown and E. Johnson, “Energy Dissipation in Confined Masonry: A Comparative Study,” Structural Safety, vol. 23, no. 2, pp. 153–162, 2001.